

Lithium-Metal Batteries

 International Edition: DOI: 10.1002/anie.201901582
 German Edition: DOI: 10.1002/ange.201901582

Stable Conversion Chemistry-Based Lithium Metal Batteries Enabled by Hierarchical Multifunctional Polymer Electrolytes with Near-Single Ion Conduction

 Dong Zhou⁺, Anastasia Tkacheva⁺, Xiao Tang, Bing Sun, Devaraj Shanmukaraj, Peng Li, Fan Zhang, Michel Armand, and Guoxiu Wang*

Abstract: The low Coulombic efficiency and serious safety issues resulting from uncontrollable dendrite growth have severely impeded the practical applications of lithium (Li) metal anodes. Herein we report a stable quasi-solid-state Li metal battery by employing a hierarchical multifunctional polymer electrolyte (HMPE). This hybrid electrolyte was fabricated via *in situ* copolymerizing lithium 1-[3-(methacryloyloxy)propylsulfonyl]-1-(trifluoromethanesulfonyl)imide (LiMTFSI) and pentaerythritol tetraacrylate (PETEA) monomers in traditional liquid electrolyte, which is absorbed in a poly(3,3-dimethylacrylic acid lithium) (PDAALi)-coated glass fiber membrane. The well-designed HMPE simultaneously exhibits high ionic conductivity ($2.24 \times 10^{-3} \text{ S cm}^{-1}$ at 25 °C), near-single ion conducting behavior (Li ion transference number of 0.75), good mechanical strength and remarkable suppression for Li dendrite growth. More intriguingly, the cation permselective HMPE efficiently prevents the migration of negatively charged iodine (I) species, which provides the as-developed Li-I batteries with high capacity and long cycling stability.

Lithium (Li) metal anode is regarded as the “holy grail” for next-generation energy storage systems due to its lowest redox potential (−3.040 V vs. standard hydrogen electrode) and high theoretical specific capacity (3860 mAhg^{−1}).^[1] Furthermore, Li metal anodes could realize novel conversion chemistry-based Li battery systems with unlithiated cathodes (e.g., lithium-oxygen (Li-O₂), lithium-sulfur (Li-S), and lithium-iodine (Li-I) batteries), which deliver much higher energy densities compared with conventional Li-ion batteries

based on Li⁺ ions intercalating cathode and anode materials.^[2] However, the Li dendrite growth during repeated Li plating/stripping not only causes great safety concerns such as short circuits and thermal runaway, but also leads to a continuous damage/regeneration of the solid electrolyte interface (SEI) upon cycling, which significantly decreases the Coulombic efficiency of Li metal batteries.^[3] In the case of conversion chemistry-based Li metal batteries, the interfacial reactions on the Li anode are more complicated due to the shuttling of soluble intermediate products (oxygen species, polysulfides, iodine species, etc.). These intermediates result in a degraded SEI with high resistance and large activation energy,^[4] and simultaneously corrode the Li metal anode, thus leading to an irreversible capacity loss.^[5] Consequently, the immobilization of such soluble intermediates can not only enhance the retention of cathode capacity, but also benefit the development of a dendrite-free Li interface.

In recent years, extensive efforts have been devoted to restraining dendrite growth on Li metal anodes. These include applying three-dimensional Li hosts,^[6] protective coating on Li metal,^[7] employing dendrite-free separators or interlayers,^[8] stabilizing the SEI by optimizing liquid electrolytes,^[9] salts^[10] or electrolyte additives,^[11] and replacing liquid electrolytes with inorganic solid electrolytes or polymer electrolytes,^[12] etc. Among the above-mentioned methods, the application of polymer electrolytes is of particular interest due to their unique merits such as flexible processability, low flammability, high tolerance to mechanical deformation, and better electrode/electrolyte interfacial properties compared with inorganic solid electrolytes.^[13] To date, two kinds of polymer electrolytes are widely employed in the research of Li metal batteries, that is, all-solid-state single-ion conducting polymer electrolytes (SIPES)^[14] and crosslinked gel polymer electrolytes (CGPEs).^[15] In the SIPES, the anions are covalently bonded to the polymer backbones, and only the counter Li⁺ cations dominate the charge flow. Therefore, the large electric fields from anion mobility can be greatly reduced, thus leading to a stable Li electrodeposition.^[16] However, to date, the existing SIPES generally suffer from low ionic conductivity ($< 10^{-5} \text{ S cm}^{-1}$ at 25 °C), which limits their application in Li metal batteries. In contrast, the CGPEs exhibit satisfactory ionic conductivity values ($> 10^{-4} \text{ S cm}^{-1}$ at 25 °C) and better electrode/electrolyte interfacial properties due to the existence of organic solvents as plasticizers. Furthermore, the crosslinking networks can facilitate a relatively homogeneous Li⁺ ion flux and accommodate the volumetric changes of Li deposition, and thus block dendrite

[*] Dr. D. Zhou,^[†] A. Tkacheva,^[†] X. Tang, Dr. B. Sun, F. Zhang, Prof. Dr. G. Wang
 Centre for Clean Energy Technology, School of Mathematical and Physical Sciences, University of Technology Sydney
 Sydney, NSW 2007 (Australia)
 E-mail: Guoxiu.Wang@uts.edu.au

Dr. D. Shanmukaraj, Prof. M. Armand
 CIC ENERGIGUNE
 Parque Tecnológico de Álava, Miñano 01510 (Spain)

Dr. P. Li
 College of Material Science and Engineering, Nanjing University of Aeronautics and Astronautics
 Nanjing 210006 (P. R. China)

[†] These authors contributed equally to this work.

 Supporting information and the ORCID identification number(s) for the author(s) of this article can be found under:
 <https://doi.org/10.1002/anie.201901582>

growth.^[15b,17] However, the CGPEs have to face a trade-off between their conductivity and mechanical strength.^[18] In addition, the polymer matrices in CGPEs usually exhibit only weak interaction with the intermediate products in conversion chemistry-based batteries, which is insufficient to restrain their shuttling.^[19] Therefore, it remains a challenging task to develop suitable polymer electrolytes for conversion chemistry-based Li metal batteries.

Herein, we report a new type of hierarchical multifunctional polymer electrolyte (HMPE) that integrates the merits of both SIPEs and CGPEs. This hybrid electrolyte is composed of an in situ prepared (1-[3-(methacryloyloxy)propylsulfonyl]-1-(trifluoromethanesulfonyl)imide (LiMTFSI)-pentaerythritol tetraacrylate (PETEA))-based CGPE in a poly(3,3-dimethylacrylic acid lithium) (PDAALi)-coated glass fiber (GF) membrane. The PDAALi-coated membrane provides the HMPE with enough mechanical strength; meanwhile, the LiMTFSI-PETEA copolymer network keeps it in a quasi-solid state without the safety risk from electrolyte leakage. Owing to the single ion conductor-containing hierarchical polymer structure, the as-developed HMPE delivers a high ionic conductivity ($2.24 \times 10^{-3} \text{ Scm}^{-1}$), a high Li ion transference number (0.75), and effective inhibition of Li dendrite growth at room temperature. When applied in Li-I batteries as a typical conversion chemistry-based system, the HMPE acts as an efficient barrier against the diffusion of iodine (I) species via electrostatic repulsion, thus resulting in a high battery capacity with long cycle life without the need for LiNO₃ additive.

Figure 1 illustrates the preparation route of HMPE. Firstly, 3,3-dimethylacrylic acid lithium (DDALi) monomer was polymerized on the surface of a GF membrane in aqueous solution (Figure 1, upper left panels; the polymerization mechanism is shown in Figure S1a in the Supporting Information). The weight increase was $\approx 22.0 \text{ wt} \%$ after PDAALi coating. It should be noted that the PDAALi is insoluble in ether-based electrolyte solvents. Subsequently, 6 wt % LiMTFSI monomer (Figures S1 b, S2 in the Supporting Information) and 2 wt % PETEA crosslinker together with 0.1 wt % hydroxy-2-methyl-1-phenyl-1-propanone (HMPP) photo-initiator were dissolved in 1M bis(trifluoromethane) sulfonamide lithium (LiTFSI) in 1,2-dioxolane

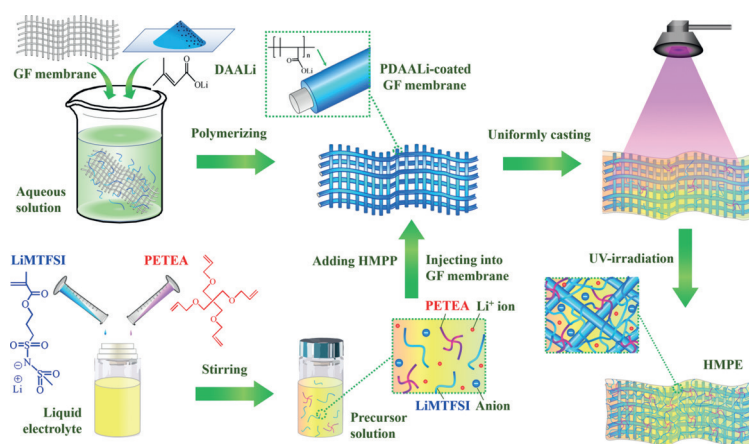


Figure 1. Schematic illustration of the preparation of HMPE.

(DOL): dimethoxymethane (DME) (1: 1 by volume) liquid electrolyte (LE) to form a precursor solution (Figure 1, lower left panels). The precursor solution was injected into the PDAALi-coated GF membrane, and then exposed to a ultraviolet (UV)-irradiation to initiate an in situ radical polymerization of C=C bonds on the LiMTFSI and PETEA molecules (Figure 1, upper right panels; the polymerization mechanism is shown in Figure S1c). During this process, a CGPE composed of polymerized LiMTFSI-PETEA framework filled with LE was formed in the PDAALi-coated GF membrane, and hence the target HMPE was obtained (Figure 1, lower right panels). It is noticed that the employment of PETEA crosslinker not only introduces a robust chemical crosslinked structure in the HMPE, but also enables a cost-efficient gelation of LE with a small amount of monomer addition (8 wt %).

When integrating the PDAALi-coated GF membrane (Figure S3) with the (LiMTFSI-PETEA)-based CGPE (the inset of Figure 2a), a homogenous HMPE film with good flexibility was developed (Figure 2a). The Fourier-transform infrared spectra (FTIR) in Figure S4 verify the successful polymerization of monomers in the HMPE. Figure 2b shows the stress-strain curves of the HMPE membrane. The HMPE can sustain a fracture stress of 4.7 MPa with a maximal strain of 7.1 %, which is dramatically higher than the GF membrane (2.9 MPa and 4.8 %). This excellent mechanical property of HMPE is essential for the assembly requirement of Li metal batteries. The HMPE also possesses much improved thermal/electrochemical stabilities and safety compared with ether-based LE (Figures S5,6).

We have measured the ionic conductivities of different electrolyte samples at a temperature range from 0 to 90 °C. As shown in Figure 2c and the Vogel-Tamman-Fulcher (VTF) fitting results in Table S1, the (LiMTFSI-PETEA)-based CGPE presents a high ionic conductivity of $6.99 \times 10^{-3} \text{ Scm}^{-1}$ at 25 °C, only slightly lower than that of the 1M LiTFSI in DOL: DME LE ($1.09 \times 10^{-2} \text{ Scm}^{-1}$) even though the polymerized LiMTFSI-PETEA matrix is a poor ionic conductor. When integrated with the PDDALi-coated GF membrane, the HMPE can maintain $2.24 \times 10^{-3} \text{ Scm}^{-1}$ at 25 °C, mainly due to the high LE uptake ability of the PDDALi-coated GF membrane (629.5 %, Figure S7). Such a high ionic conductivity is sufficient to meet the need for practical Li metal batteries.

Lithium ion transference number (t_{Li}^+) is an important property for polymer electrolytes, since a high t_{Li}^+ will contribute to reduced concentration polarization and improved rate performance of batteries.^[20] As shown in Figure 2d, the t_{Li}^+ of HMPE reaches 0.75, which is notably higher than that of the LE absorbed in GF membrane (0.34, Figure S8a) and LE absorbed in PDAALi-coated GF membrane (0.54, Figure S8b). This phenomenon has been further elucidated by density functional theory (DFT) calculations. It has been revealed that during the solvation process in DOL/DME-based electrolytes, Li⁺ ions tend to interact with O atoms on the DME molecules with high solvating ability, and form stable Li⁺(DME)₃

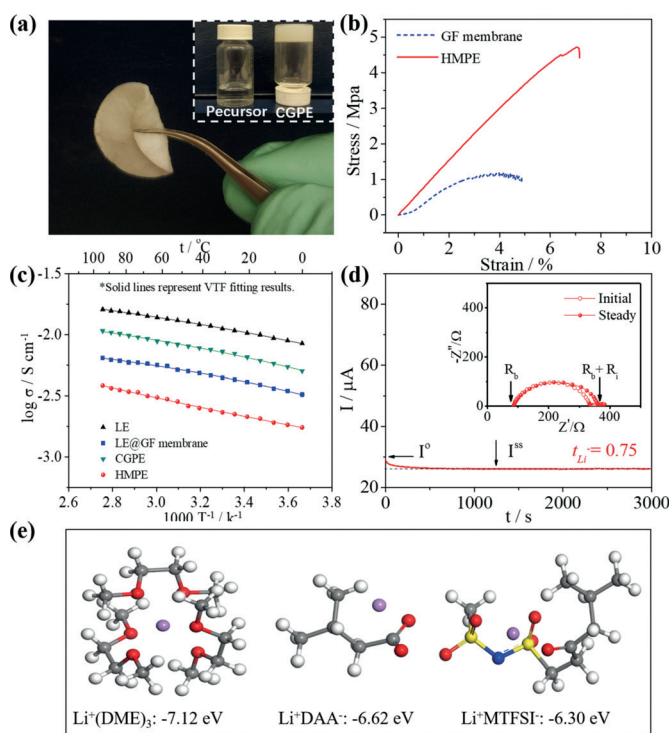


Figure 2. Characterization of HMPE. a) Optical images of HMPE film. The images of the precursor solution and the CGPE are shown in the inset. b) Stress-strain curves of the pristine GF membrane and HMPE film at 1 mm min^{-1} ; c) Ionic conductivities of the LE, LE absorbed in GF membrane, CGPE and HMPE versus temperature. The plots represent the experimental data while the solid lines represent VTF fitting results. d) The chronoamperometry profile of Li|HMPE|Li cells under a polarization voltage of 10 mV, and the corresponding electrochemical impedance spectra (EISs) before and after polarization (inset). e) Calculated complexation energies of the $\text{Li}^+(\text{DME})_3$, Li^+DAA^- and $\text{Li}^+\text{MTFSI}^-$. Purple, gray, white, red, blue and yellow balls represent lithium, carbon, hydrogen, oxygen, nitrogen and sulfur atoms, respectively.

solvation complexes.^[21] As shown in Figure 2e, the solvation energy of $\text{Li}^+(\text{DME})_3$ is calculated to be -7.12 eV , which is much higher than the dissociation energy of Li^+DAA^- (-6.62 eV) and $\text{Li}^+\text{MTFSI}^-$ (-6.30 eV). As a result, in the HMPE, Li^+ ions preferentially dissociate from the single ion conducting PDAALi coating layer and polymerized LiMTFSI-PETEA framework, and subsequently solvate in the DME solvent. These additional solvated Li^+ ions would greatly improve the t_{Li}^+ of electrolyte and lead to a near-single ion conducting behavior, which is coincident with the above-mentioned experimental results.

Galvanostatic cycling performances of symmetric Li|Li cells at 1 mA cm^{-2} were measured to investigate the compatibility of HMPE with the Li metal electrodes. For the cell using LiNO_3 -free 1 M LiTFSI in DOL:DME electrolyte and GF membrane separator, the overpotential of significantly increases with the cycling time due to the accumulated thick SEI, and then suddenly drops at around 240 h, indicating a short-circuit caused by dendrite growth (Figure 3a).^[16,19] The Li|HMPE|Li cell, however, maintains a low and stable voltage hysteresis without obvious oscillation (Figure 3a and Figures S9, S10). These results demonstrate that the HMPE

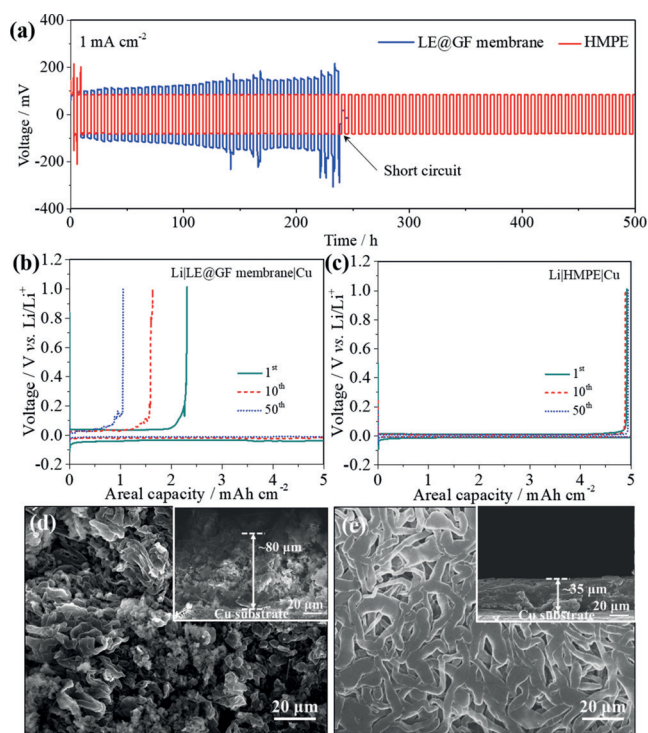


Figure 3. a) Galvanostatic cycling curves of Li|Li symmetrical cells using LE absorbed in GF membrane or HMPE at 1 mA cm^{-2} with a cut-off capacity of 3 mAh cm^{-2} ; Voltage profiles of the Li plating/stripping process in b) Li|LE@GF membrane|Cu and c) Li|HMPE|Cu cells at a current density of 0.5 mA cm^{-2} with a capacity limitation of 5 mAh cm^{-2} . Top and cross-sectional (shown in insets) FE-SEM images of Li deposition obtained by plating 5 mAh cm^{-2} Li on Cu substrate at 0.5 mA cm^{-2} in d) Li|LE@GF membrane|Cu and e) Li|HMPE|Cu cells.

endows a homogenous Li deposition without the safety hazard from dendrite growth.

Li|Cu cells were applied to further evaluate the Coulombic efficiencies of Li plating/stripping (the ratio of Li stripping capacity to Li plating capacity) in different electrolytes. In each cycle, Li metal was firstly plated on Cu current collectors with a capacity limitation of 5 mAh cm^{-2} at 0.5 mA cm^{-2} , and then stripped to 1.0 V at the same current density. As shown in Figure 3b, in the cell using LE with a GF separator membrane, the initial Li stripping capacity is much lower than the plating capacity (46.2%), and rapidly decreases with the increased cycle number. The Coulombic efficiency is only 21.0% in the 50th cycle, which implies a large amount of irreversible capacity loss. For comparison, the Li plating/stripping processes of the Li|HMPE|Cu cell is highly stable and reversible throughout cycling (Figure 3c). The corresponding Coulombic efficiency attains 98.3% after 100 cycles (Figure S11). Moreover, for the cell using HMPE, the hysteresis of the voltage plateaus between Li plating and stripping in the 50th cycle is only $\approx 10.8 \text{ mV}$, which is much lower than that using the LE with a GF separator membrane ($\approx 47.2 \text{ mV}$), suggesting a low polarization in the HMPE-based cells.

The morphologies of Li deposits on Cu substrates with a plating capacity of 5 mAh cm^{-2} were investigated by field

emission scanning electron microscope (FE-SEM) images. In the cell using LE with a GF separator membrane, a highly loose and porous plating structure with numerous Li dendrites is observed (Figure 3d). Furthermore, it is noted that the thickness of the Li deposited layer is $\approx 80 \mu\text{m}$ (Figure 3d, inset), far exceeding the theoretical thickness value ($\approx 24 \mu\text{m}$). This is consistent with its low Coulombic efficiencies as noted in Figure 3b. In contrast, the Li deposit in the Li|HMPE|Cu cell exhibits a morphology resembling compactly aggregated nodule-like particles ($\approx 7 \mu\text{m}$) without dendrite formation (Figure 3e). The thickness of the Li layer deposited in the HMPE is only $\approx 35 \mu\text{m}$, which is close to the theoretical value (Figure 3e, inset). Such a compact Li deposition with low surface area in HMPE can significantly mitigate the interfacial side reactions with electrolytes, and hence results in high Coulombic efficiency, long cycle life, and safety-reinforcement against short-circuiting.

The significant inhibition effect of HMPE on dendrite growth can be explained as follows. In plating process of Li metal cells using traditional LE with a GF separator membrane, Li^+ ions prefer to diffuse to the defects on the SEI (where the local current density is increased) and concentrate in the vicinity, and then grow into Li dendrites (Figure S12, upper panels).^[22] Moreover, The low t_{Li^+} of traditional LE results in a depletion of mobile anions near the Li plating side, which in turn triggers a large electric field and accelerates the growth of Li dendrites (i.e., a decrease in Sand's time based on Equation S4).^[16] In contrast, in Li metal cells using HMPE, the crosslinking polymerized LiMTFSI-PETEA network can not only generate a relatively homogeneous Li^+ flux and retard Li^+ ions from becoming depleted around the defects on the SEI, but also efficiently ease the volumetric changes during Li deposition, thus restraining any incipient dendrite growth.^[23] Furthermore, the high t_{Li^+} can effectively reduce the polarization from the concentration gradient caused by anion mobility, which results in a uniform Li electrodeposition (Figure S12, lower panels). Such dual optimizing effects contribute to the superior performance of HMPE in Li metal batteries.

Li-I cells were fabricated to investigate the electrochemical characteristics of HMPE in conversion chemistry-based batteries. The permeability of I_3^- as a representative soluble iodine species was directly measured via visual observation, which was performed on H-shaped cells filled with 20 mL blank DOL: DME (1: 1 by volume) solvent in the right chamber, and 20 mL 50 mM LiI_3 in DOL: DME in the left chamber. It is seen that in the H-cell separated by a GF membrane, the I_3^- anions continuously diffuse through the GF membrane and reach the other side of the cell, which is reflected by the obvious color change of blank solvents from transparent to dark brown (Figure 4a, upper panels). However, in the cell connected by the cation permselective HMPE film, the solvent in the right chamber remains clear after 6 h (Figure 4a, lower panels), indicating the significant suppression of I_3^- migration by the HMPE via repulsive electrostatic interaction.

Figure 4b and Figure S16 show the rate performances of the Li-I cells applying graphene oxide (GO) wrapped carbon cloth (CC)-iodine (labeled as "CC-I@GO", Figure S13–15)

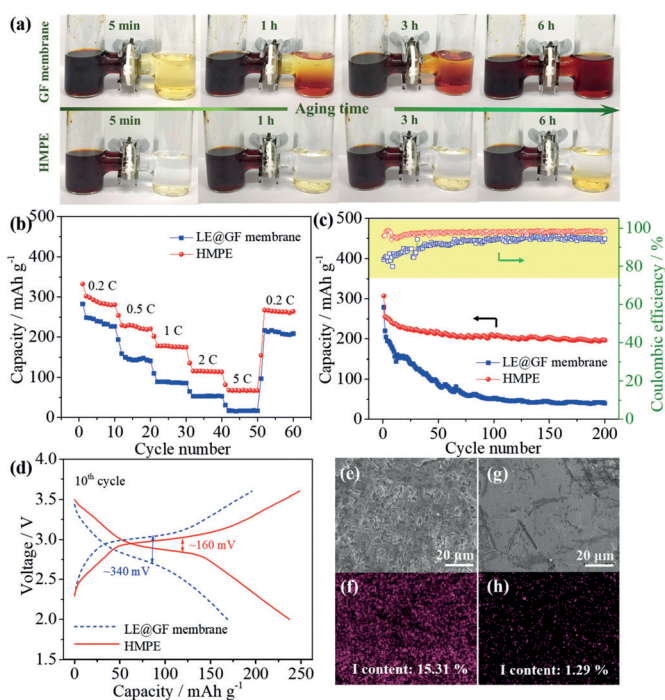


Figure 4. Electrochemical performance of quasi-solid-state Li-I batteries with HMPEs. a) Visual observation of LiI_3 transport through a GF membrane (upper panels) and a HMPE film (lower panels) at room temperature. b) Rate performances, c) cycling performances at 0.5 C, and d) charge/discharge profiles at the 10th cycle at 0.5 C of Li|LE@GF membrane|CC-I@GO and Li|HMPE|CC-I@GO cells; e, g) the morphologies and f, h) corresponding EDS mappings of iodine of Li anodes obtained from the (e, f) Li|LE@GF membrane|CC-I@GO and (g, h) Li|HMPE|CC-I@GO cells after 200 cycles at 0.5 C.

cathodes. The Li|HMPE|CC-I@GO cell delivers specific discharge capacities of 288, 228, 177, 115 and 67 mAhg^{-1} (based on the mass of iodine) at 0.2, 0.5, 1, 2 and 5 C, respectively, which is dramatically higher than the Li|LE@GF membrane|CC-I@GO cell. Figure 4c exhibits the cycling performance of Li-I cells at 0.5 C. The Li|HMPE|CC-I@GO cell delivers a superior long-term cycling stability with a discharge capacity of 196 mAhg^{-1} after 200 cycles, and the average Coulombic efficiency reaches $\approx 98\%$, which is consistent with the cyclic voltammetry (CV) result in Figure S17. In contrast, the discharge capacity of the Li|LE@GF membrane|CC-I@GO cell is only 39 mAhg^{-1} after 200 cycles with an average Coulombic efficiency of $\approx 93\%$. Furthermore, as seen from the corresponding typical discharge/charge curves in Figure 4d, the discharge/charge potential gap of the cell used HMPE ($\approx 160 \text{ mV}$) is obviously smaller than that using LE with a GF separator membrane ($\approx 340 \text{ mV}$). This suggests that the application of HMPE can remarkably reduce the polarization of Li-I batteries. The excellent electrochemical performances of the HMPE-based Li-I batteries noted above can be attributed to the effective immobilization of iodine species (I^- and I_3^-) by HMPE, and the stable electrode/HMPE interfaces upon cycling (see the EIS results in Figure S18 and Table S2).

The Li anodes disassembled from Li-I cells after 200 cycles were further characterized by FE-SEM. It is clearly

seen that massive dendrite structures and holes appear on the Li anode surface obtained from the Li|LE@GF membrane|CC-I@GO cell (Figure 4e). Meanwhile, the iodine content on such an anode is as high as 15.31 wt% (Figure 4f). After replacing the LE and GF separator membrane with HMPE, as expected, the surface of Li anode becomes smooth and the Li dendrite growth is significantly inhibited (Figure 4g). Moreover, the iodine content on the Li anode from Li|HMPE|CC-I@GO cell is only 1.29 wt% (Figure 4h), which verifies a successful blocking of the shuttle effect. As shown in Table S3, the performance of HMPE is better than previously reported representative polymer electrolytes for Li metal batteries.

In conclusion, we developed a novel hierarchical multi-functional polymer electrolyte with near-single ion conduction for Li metal batteries. This polymer electrolyte was fabricated by integrating a (LiMTFSI-PETEA)-based CGPE with a PDDALi-coated GF membrane via a facile in situ UV-initiated polymerization. The single ion conductor-containing hierarchical polymer framework provides the as-developed HMPE with high mechanical strength (4.7 MPa), ionic conductivity ($2.24 \times 10^{-3} \text{ Scm}^{-1}$) and Li ion transference number (0.75) at room temperature together with enhanced safety. More importantly, the HMPE not only allows a homogeneous Li deposition without dendrite growth, but also effectively suppresses the diffusion of iodine species, and therefore enables a stable cycling of quasi-solid-state Li-I cells. The fundamental design concept and preparation technique for the HMPE can be extended to other alkali metal battery systems based on conversion chemistry (e.g., Li-S, Li-O₂, lithium-selenium, sodium-sulfur, sodium-oxygen batteries), and open a new avenue for the development of high-performance energy storage devices.

Acknowledgements

This work was supported by Australian Renewable Energy Agency project (ARENA 2014/RND106), Rail Manufactory CRC projects (RMCRC; R1.1.1 and R1.1.2), and the Australian Research Council (ARC) Discovery Project (DP160104340 and DP170100436).

Conflict of interest

The authors declare no conflict of interest.

Keywords: hierarchical structure · iodine cathode · lithium metal battery · near-single ion conduction · polymer electrolyte

How to cite: *Angew. Chem. Int. Ed.* **2019**, *58*, 6001–6006
Angew. Chem. **2019**, *131*, 6062–6067

- [1] a) G. Zheng, S. W. Lee, Z. Liang, H.-W. Lee, K. Yan, H. Yao, H. Wang, W. Li, S. Chu, Y. Cui, *Nat. Nanotechnol.* **2014**, *9*, 618; b) J. Meng, H. Guo, C. Niu, Y. Zhao, L. Xu, Q. Li, L. Mai, *Joule* **2017**, *1*, 522–547.

- [2] P. G. Bruce, S. A. Freunberger, L. J. Hardwick, J. M. Tarascon, *Nat. Mater.* **2012**, *11*, 19–29.
- [3] H. Kim, G. Jeong, Y.-U. Kim, J.-H. Kim, C.-M. Park, H.-J. Sohn, *Chem. Soc. Rev.* **2013**, *42*, 9011–9034.
- [4] D. Su, D. Zhou, C. Wang, G. Wang, *Adv. Funct. Mater.* **2018**, *28*, 1800154.
- [5] Y. Fu, Y. S. Su, A. Manthiram, *Angew. Chem. Int. Ed.* **2013**, *52*, 6930–6935; *Angew. Chem.* **2013**, *125*, 7068–7073.
- [6] a) K. Yan, B. Sun, P. Munroe, G. Wang, *Energy Storage Mater.* **2018**, *11*, 127–133; b) C. Zhang, S. Liu, G. Li, C. Zhang, X. Liu, J. Luo, *Adv. Mater.* **2018**, *30*, 1801328; c) S.-H. Wang, Y.-X. Yin, T.-T. Zuo, W. Dong, J.-Y. Li, J.-L. Shi, C.-H. Zhang, N.-W. Li, C.-J. Li, Y.-G. Guo, *Adv. Mater.* **2017**, *29*, 1703729.
- [7] a) Y. Sun, Y. Zhao, J. Wang, J. Liang, C. Wang, Q. Sun, X. Lin, K. R. Adair, J. Luo, D. Wang, R. Li, M. Cai, T.-K. Sham, X. Sun, *Adv. Mater.* **2019**, *31*, 1806541; b) J. Liang, X. Li, Y. Zhao, L. V. Goncharova, G. Wang, K. R. Adair, C. Wang, R. Li, Y. Zhao, Y. Qian, L. Zhang, R. Yang, S. Lu, X. Sun, *Adv. Mater.* **2018**, *30*, 1804684; c) Q. Pang, L. Zhou, L. F. Nazar, *Proc. Natl. Acad. Sci. USA* **2018**, *115*, 12389–12394.
- [8] a) N. B. Aetukuri, S. Kitajima, E. Jung, L. E. Thompson, K. Virwani, M. L. Reich, M. Kunze, M. Schneider, W. Schmidbauer, W. W. Wilcke, *Adv. Energy Mater.* **2015**, *5*, 1500265; b) Y. Lu, M. Tikekar, R. Mohanty, K. Hendrickson, L. Ma, L. A. Archer, *Adv. Energy Mater.* **2015**, *5*, 1402073.
- [9] a) J. Heine, P. Hilbig, X. Qi, P. Niehoff, M. Winter, P. Bieker, *J. Electrochem. Soc.* **2015**, *162*, A1094–A1101; b) M. S. Park, S. B. Ma, D. J. Lee, D. Im, S.-G. Doo, O. Yamamoto, *Sci. Rep.* **2014**, *4*, 3815.
- [10] a) J. Qian, W. A. Henderson, W. Xu, P. Bhattacharya, M. Engelhard, O. Borodin, J.-G. Zhang, *Nat. Commun.* **2015**, *6*, 6362; b) Y. Lu, Z. Tu, L. A. Archer, *Nat. Mater.* **2014**, *13*, 961–969.
- [11] a) D. Aurbach, E. Pollak, R. Elazari, G. Salitra, C. S. Kelley, J. Affinito, *J. Electrochem. Soc.* **2009**, *156*, A694–A702; b) J. Jeong, J.-N. Lee, J.-K. Park, M.-H. Ryou, Y. M. Lee, *Electrochim. Acta* **2015**, *170*, 353–359.
- [12] a) D. Zhou, R. Liu, Y. B. He, F. Li, M. Liu, B. Li, Q. H. Yang, Q. Cai, F. Kang, *Adv. Energy Mater.* **2016**, *6*, 1502214; b) X.-X. Zeng, Y.-X. Yin, N.-W. Li, W.-C. Du, Y.-G. Guo, L.-J. Wan, *J. Am. Chem. Soc.* **2016**, *138*, 15825–15828.
- [13] L. Yue, J. Ma, J. Zhang, J. Zhao, S. Dong, Z. Liu, G. Cui, L. Chen, *Energy Storage Mater.* **2016**, *5*, 139–164.
- [14] a) R. Bouchet, S. Maria, R. Mezziane, A. Aboulaich, L. Lienafa, J.-P. Bonnet, T. N. Phan, D. Bertin, D. Gimes, D. Devaux, *Nat. Mater.* **2013**, *12*, 452; b) Q. Ma, H. Zhang, C. Zhou, L. Zheng, P. Cheng, J. Nie, W. Feng, Y. S. Hu, H. Li, X. Huang, *Angew. Chem. Int. Ed.* **2016**, *55*, 2521–2525; *Angew. Chem.* **2016**, *128*, 2567–2571; c) S. Li, A. I. Mohamed, V. Pande, H. Wang, J. Cuthbert, X. Pan, H. He, Z. Wang, V. Viswanathan, J. F. Whitacre, *ACS Energy Lett.* **2018**, *3*, 20–27.
- [15] a) H. Wu, Y. Cao, H. Su, C. Wang, *Angew. Chem. Int. Ed.* **2018**, *57*, 1361–1365; *Angew. Chem.* **2018**, *130*, 1375–1379; b) S. Choudhury, R. Mangal, A. Agrawal, L. A. Archer, *Nat. Commun.* **2015**, *6*, 10101; c) X. Lei, X. Liu, W. Ma, Z. Cao, Y. Wang, Y. Ding, *Angew. Chem. Int. Ed.* **2018**, *57*, 16131–16135; *Angew. Chem.* **2018**, *130*, 16363–16367.
- [16] H. Zhang, C. Li, M. Piszcz, E. Coya, T. Rojo, L. M. Rodriguez-Martinez, M. Armand, Z. Zhou, *Chem. Soc. Rev.* **2017**, *46*, 797–815.
- [17] Z. Liang, G. Zheng, C. Liu, N. Liu, W. Li, K. Yan, H. Yao, P.-C. Hsu, S. Chu, Y. Cui, *Nano Lett.* **2015**, *15*, 2910–2916.
- [18] D. Zhou, R. Liu, J. Zhang, X. Qi, Y.-B. He, B. Li, Q.-H. Yang, Y.-S. Hu, F. Kang, *Nano Energy* **2017**, *33*, 45–54.
- [19] L. Ma, P. Nath, Z. Tu, M. Tikekar, L. A. Archer, *Chem. Mater.* **2016**, *28*, 5147–5154.

- [20] H.-D. Nguyen, G.-T. Kim, J. Shi, E. Paillard, P. Judeinstein, S. Lyonnard, D. Bresser, C. Iojoiu, *Energy Environ. Sci.* **2018**, *11*, 3298–3309.
- [21] a) Q. Zhang, Y. Lu, L. Miao, Q. Zhao, K. Xia, J. Liang, S. L. Chou, J. Chen, *Angew. Chem. Int. Ed.* **2018**, *57*, 14796–14800; *Angew. Chem.* **2018**, *130*, 15012–15016; b) C. C. Su, M. He, R. Amine, Z. Chen, K. Amine, *Angew. Chem. Int. Ed.* **2018**, *57*, 12033–12036; *Angew. Chem.* **2018**, *130*, 12209–12212.
- [22] D. Aurbach, E. Zinigrad, Y. Cohen, H. Teller, *Solid State Ionics* **2002**, *148*, 405–416.
- [23] S. Choudhury, D. Vu, A. Warren, M. D. Tikekar, Z. Tu, L. A. Archer, *Proc. Natl. Acad. Sci. USA* **2018**, *115*, 6620.

Manuscript received: February 5, 2019
Revised manuscript received: February 26, 2019
Accepted manuscript online: March 4, 2019
Version of record online: March 26, 2019